ACS OMEGA

http://pubs.acs.org/journal/acsodf

Article

Preparation of a Tetra-Imidazolium Salt and Sensing for *p*-Dinitrobenzene

Zhi-Xiang Zhao, Yuan-Yuan Wu, Dong-Xue Zhao, and Qing-Xiang Liu*

Cite This: *ACS Omega* 2023, 8, 6869−6874

Read Online

ACCESS | Metrics & More | Article Recommendations | Supporting Information

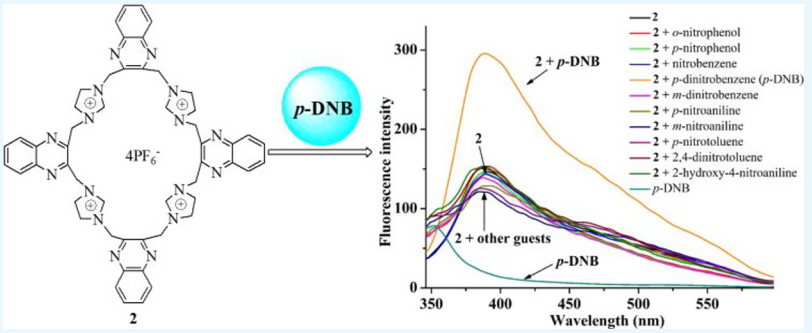

ABSTRACT: A macrocyclic tetra-imidazolium salt (**2**) based on quinoxaline was prepared and characterized. The recognition of **2** to nitro compounds was investigated by fluorescence spectroscopy, ^{1}H NMR titrations, MS, IR spectroscopy, and UV/vis spectroscopy. The results displayed that **2** was able to effectively differentiate *p*-dinitrobenzene from other nitro compounds via the fluorescence method.

1. INTRODUCTION

The detection of nitroaromatics in recent years has attracted extensive attention because these types of compounds are explosive, posing a threat to public safety.[1−10] Compared with traditional detection methods (such as LC−MS, GC−MS, and HPLC),[11−13] the fluorescence method has some advantages, such as high sensitivity, speediness, and easy operation.[14−18] Among these chemosensors, the forces acting between the host and guest are mostly hydrogen bonds (such as N−H···O, O−H···O, and C−H···O). Hence, it is a meaningful work to design and synthesize hosts with active hydrogen atoms.

To search for a suitable chemosensor with active hydrogen atoms, herein, we designed and synthesized a macrocyclic tetra-imidazolium salt (**2**) based on quinoxaline. The hydrogen atoms on the imidazolium salt (NC*H*N) of **2** can capture guests through the formation of hydrogen bonds. The selective recognition of **2** to nitroaromatics was researched through fluorescence spectroscopy, ^{1}H NMR titrations, MS, IR spectroscopy, and UV/vis spectroscopy.

2. EXPERIMENTAL METHODOLOGY

2.1. Chemicals and Apparatus. All chemicals used for the experimental research were of reagent grade. The melting points were measured using a Boetius block device. A PerkinElmer spectra 100 FT-IR spectrophotometer was applied for the analysis of the infrared spectra. A Varian spectrometer was applied for ^{1}H NMR and ^{13}C NMR spectra. A PerkinElmer 2400C elemental analyzer was applied to carry out elemental analyses. The luminescence spectra were measured, applying a Shimadzu RF-5301PC luminescence spectrophotometer. A VG ZAB-HS mass spectrometer was applied to measure the mass spectra.

2.2. Synthesis of 1,4-Dibromo-2,3-butanedione. A mixture of liquid bromine (18.720 g, 117.0 mmol) and chloroform (10 mL) was added dropwise to another mixture of 2,3-butanedione (5.086 g, 59.0 mmol) and chloroform (10 mL) with stirring at 25 °C. After the addition was completed, the reaction temperature was raised to refluxing until no hydrogen bromide was released; then, the reaction was stopped. After cooling, the reaction system was poured into a beaker with ice water and placed for 1 h. 1,4-Dibromo-2,3-butanedione was obtained via filtration and recrystallization with chloroform (20.0 × 2 mL). Yield: 10.043 g (71%). M.p: 116−117 °C. ^{1}H NMR (400 MH_Z, $CDCl_3$): δ 4.32 (s, 4H, CH_2).

2.3. Preparation of 2,3-Bis(bromomethyl)-quinoxaline. A mixture of ethanol (26 mL) and 1,4-dibromo-2,3-butanedione (2.024 g, 8.3 mmol) was added to another mixture of 1,2-diaminobenzene (0.898 g, 8.3 mmol)

Received: November 27, 2022
Accepted: January 18, 2023
Published: February 9, 2023

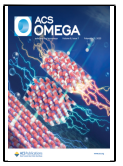

Scheme 1. Preparation of 2

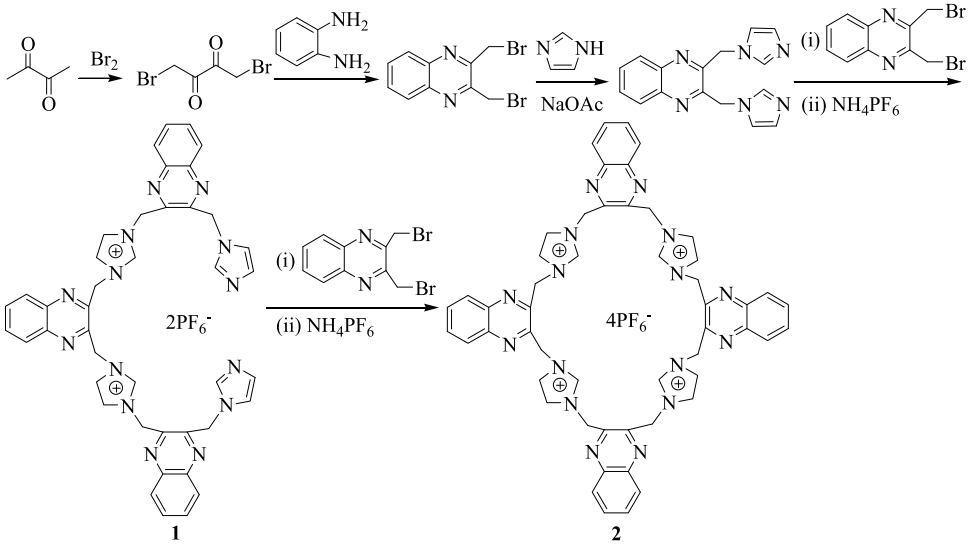

and ethanol (25 mL) at 0 °C. After 3 h, the precipitate was collected through filtration and washed with ethyl ether. 2,3-Bis(bromomethyl)quinoxaline was obtained as a white powder. Yield: 2.302 g (88%). M.p: 155−156 °C. ^{1}H NMR (400 MH$_Z$, DMSO-d_6): δ 4.92 (s, 4H, CH_2), 7.79−7.81 (m, 2H, ArH), 8.07−8.11 (m, 2H, ArH).

2.4. Preparation of 2,3-Bis(1-imidazol-1′-yl)-quinoxaline. A THF (100 mL) suspension of imidazole (0.950 g, 14.6 mmol) and anhydrous sodium acetate (1.720 g, 21.0 mmol) was stirred for 1 h under refluxing. Then, 2,3-bis(bromomethyl)quinoxaline (1.120 g, 3.6 mmol) was added dropwise to the above reaction flask and continually stirred for 4 h. The mixture was filtered, the filtrate was concentrated to 4 mL, and a small amount of ethyl ether was added to afford a solid. 2,3-Bis(1-imidazol-1′-yl)quinoxaline was obtained via filtration and washed with water. Yield: 0.710 g (70%). M.p: 196−198 °C. ^{1}H NMR (400 MH$_Z$, DMSO-d_6): δ 5.69 (s, 4H, CH_2), 6.97 (s, 2H, ArH), 7.17 (s, 2H, ArH), 7.77 (s, 2H, imi$H$), 7.81−7.85 (m, 2H, ArH), 7.94−7.97 (m, 2H, ArH) (imi = imidazole).

2.5. Preparation of Compound 1. A THF (50.0 mL) solution of 2,3-bis(bromomethyl)quinoxaline (0.060 g, 0.19 mmol) and 2,3-bis(1-imidazol-1′-yl)quinoxaline (3.480 g, 12.0 mmol) reacted for 4 days at 30 °C, and a white solid was generated. The solid was obtained through filtration. Then, a methanol (10.0 mL) solution of NH_4PF_6 (0.101 g, 0.62 mmol) was added to the methanol (20.0 mL) solution of this solid with stirring, and a white powder was immediately generated. Compound **1** was obtained by filtration and dried in a vacuum. Yield: 0.120 g (58%). M.p: > 300 °C. ^{1}H NMR (400 MH$_Z$, DMSO-d_6): δ 9.47 (s, 2H, imi$H$), 8.05 (d, J = 7.6 Hz, 2H, imi$H$), 7.91−7.92 (m, 12H, ArH), 7.85 (s, 4H, imi$H$), 7.28 (s, 2H, imi$H$), 7.03 (s, 2H, imi$H$), 6.16 (s, 4H, CH_2), 6.12 (s, 4H, CH_2), 5.79 (s, 4H, CH_2). Anal. Calcd for $C_{42}H_{36}N_{14}P_2F_{12}$: C, 49.13; H, 3.53; N, 19.09%. Found: C, 49.31; H, 3.44; N, 19.17%.

2.6. Preparation of Compound 2. A CH_3CN (25.0 mL) solution of 2,3-bis(bromomethyl)quinoxaline (0.030 g, 0.1 mmol) and **1** (0.110 g, 0.1 mmol) reacted for 4 days under refluxing, and a white solid was generated. This solid was obtained through filtration. Then, the methanol (20.0 mL) solution of this solid was added to methanol (10.0 mL) of NH_4PF_6 (0.200 g, 1.2 mmol), and a white powder was generated. Compound **2** was obtained by filtration and dried in a vacuum. Yield: 0.060 g (41%). M.p: > 300 °C. ^{1}H NMR (400 MHz, DMSO-d_6): δ 9.59 (s, 4H, imi$H$), 8.05 (d, J = 8.0 Hz, 8H, imi$H$) 7.92−7.99 (m, 8H, ArH), 7.86−7.90 (m, 8H, ArH), 6.15 (s, 16H, CH_2). ^{13}C NMR (100 MHz, DMSO-d_6): δ 148.0 (ArC), 145.8 (ArC), 141.8 (imi$C$), 140.2 (ArC), 137.9 (ArC), 135.4 (ArC), 131.1 (ArC), 128.4 (ArC), 124.0 (ArC), 123.7 (ArC), 113.2 (ArC), 112.3 (ArC), 112.2 (ArC), 50.4 (CH_2). Anal. Calcd for $C_{52}H_{44}N_{16}P_4F_{24}$: C, 42.40; N, 15.22; H, 3.01%. Found: C, 42.38; N, 15.34; H, 3.25%.

2.7. Fluorescence Titrations. Host **2** was dissolved in CH_2Cl_2/DMSO (v:v = 199:1) to prepare the stock solution (1.0×10^{-4} M). The guests were dissolved in CH_2Cl_2 to prepare the stock solutions of guests (5.0×10^{-4} mol/L). Different amounts of guest solutions and 0.5 mL of the host solution were added to a 10 mL volumetric flask and then diluted to 10 mL to form the sample solutions. The concentrations of the guests were 0−15.0×10^{-6} M, and the concentration of the host was 5.0×10^{-6} M for the sample solution. A quartz cuvette with 1 cm path-length was used for host **2** to record the fluorescence emission spectra, which ranged from 345 to 595 nm (the excitation slits at 15 nm and emission at 15 nm). The excitation wavelength was 318 nm. All tests were accomplished at room temperature. The data of processing and analysis were carried out using Origin 8.0. Freshly distilled CH_2Cl_2 and DMSO were used in the titrations.

2.8. Method for Job's Plot. The stock solution was prepared according to a method similar to the fluorescence experiment. In the measuring solutions, the mole fractions of the guest were varied from 0 to 1, and the total concentration was fixed at 5.0×10^{-6} M. A quartz cuvette with 1 cm path-length was used for host **2** to record the fluorescence emission spectra. All tests were accomplished at room temperature. The data of processing and analysis were carried out using Origin 8.0.

3. RESULTS AND DISCUSSION

3.1. Synthesis and Characterization of Tetra-Imidazolium Salt 2. The reaction of 2,3-butanedione with bromine afforded 1,4-dibromo-2,3-butanedione, which further reacted

https://doi.org/10.1021/acsomega.2c07587
ACS Omega 2023, 8, 6869−6874

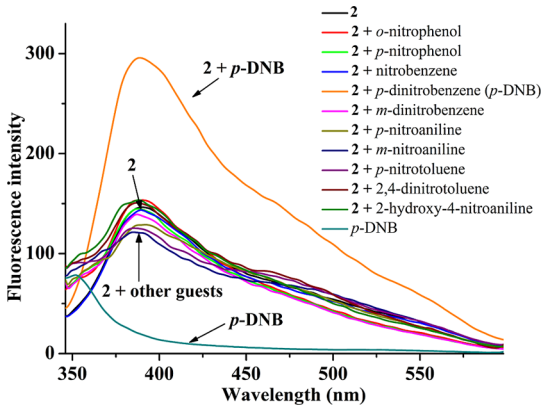

Figure 1. Fluorescence spectra of **2** (5.0×10^{-6} M) when 10 equiv of *o*-nitrophenol, *p*-nitrophenol, nitrobenzene, *p*-dinitrobenzene (*p*-DNB), *m*-dinitrobenzene, *m*-nitroaniline, *p*-nitroaniline, *p*-nitrotoluene, 2,4-dinitrotoluene, and 2-hydroxy-4-nitroaniline in CH_2Cl_2/DMSO (v:v = 199:1) was added at ambient temperature (λ_{ex} = 318 nm).

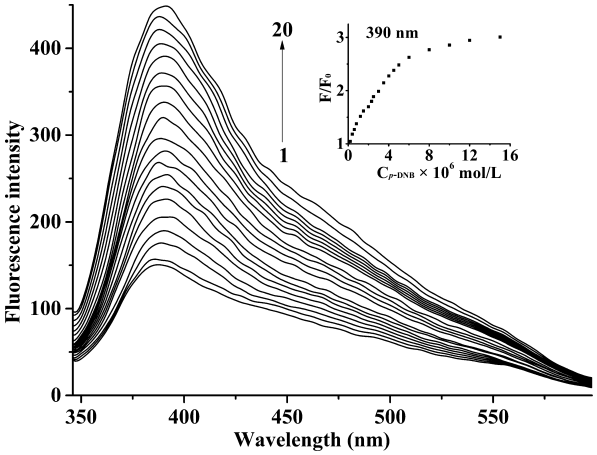

Figure 2. Fluorescence titration spectra of **2** (5.0×10^{-6} M) in the presence of various $C_{p\text{-DNB}}$ in CH_2Cl_2/DMSO at ambient temperature. $C_{p\text{-DNB}}$ for curves 1−20 are 0.0, 0.2, 0.4, 0.6, 0.8, 1.2, 1.5, 2.0, 2.3, 2.5, 3.0, 3.5, 4.0, 4.5, 5.0, 6.0, 8.0, 10.0, 12.0, and 15.0×10^{-6} M. Inset: the fluorescence of **2** vs $C_{p\text{-DNB}}$ at 390 nm (λ_{ex} = 318 nm).

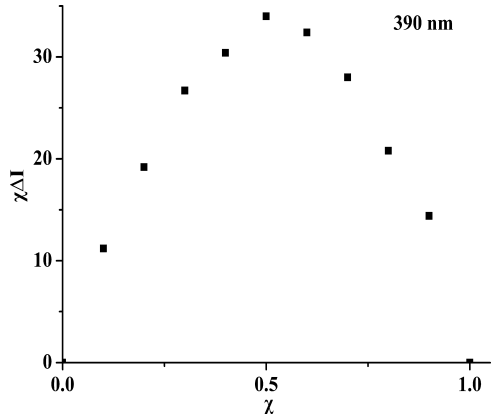

Figure 3. Job's plot for **2**·*p*-DNB in CH_2Cl_2/DMSO (v:v = 199:1) at 318 nm. The total concentration of **2** and *p*-DNB was 5.0×10^{-6} mol/L.

with 1,2-diaminobenzene to generate 2,3-bis(bromomethyl)-quinoxaline, as shown in Scheme 1. Imidazole reacted with 2,3-

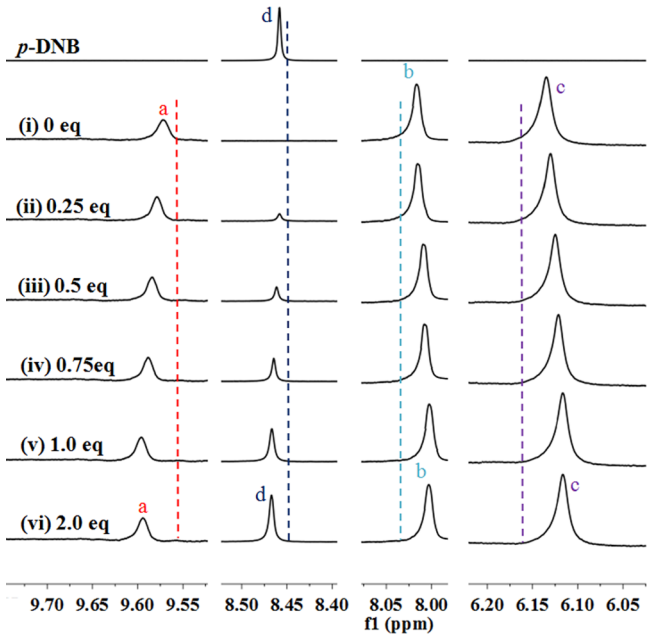

Figure 4. Part of ^{1}H NMR spectra in DMSO-d_6. (i) Free **2**; (ii) **2** and 0.25 equiv of *p*-DNB; (iii) **2** and 0.5 equiv of *p*-DNB; (iv) **2** and 0.75 equiv of *p*-DNB; (v) **2** and 1.0 equiv of *p*-DNB; (vi) **2** and 2.0 equiv of *p*-DNB.

bis(bromomethyl)quinoxaline to form 2,3-bis(1-imidazol-1′-yl)quinoxaline, which further reacted with 2,3-bis-(bromomethyl)quinoxaline to afford compound **1**. Compound **1** reacted with 2,3-bis(bromomethyl)quinoxaline, and the following anion exchange was performed using NH_4PF_6 in methanol to afford macrocyclic compound **2**.

Compound **2** was soluble in CH_3CN and DMSO but hardly soluble in petroleum ether, water, benzene and diethyl ether. The proton signal (NC*H*N) (δ = 9.59 ppm) for imidazolium in the ^{1}H NMR spectra of **2** was in line with the proton signals of known imidazolium salts.[19,20] Through referring to the literatures with structures similar to compound **2**,[21,22] we know that compound **2** is not an exactly symmetric structure, but the chemical environment of some protons is very close. Because the range of the ^{1}H NMR chemical shift is relatively small (0−10 ppm for Figure S11), some protons with a close chemical environment cannot be distinguished. As a result, the number of ^{1}H NMR signals is consistent with the symmetrical structure. By contrast, the range of ^{13}C NMR chemical shift (0−150 ppm for Figure S12) is far greater than the range of the ^{1}H NMR chemical shift, so ^{13}C NMR can distinguish some carbon atoms with a relatively close chemical environment.

3.2. Recognition of *p*-Dinitrobenzene Using Macrocycle 2 as a Chemosensor. Macrocycle **2** was chosen as a host to study the recognition ability of nitro compounds (*o*-nitrophenol, *p*-nitrophenol, nitrobenzene, *p*-dinitrobenzene (*p*-DNB), *m*-dinitrobenzene, *m*-nitroaniline, *p*-nitroaniline, *p*-nitrotoluene, 2,4-dinitrotoluene, and 2-hydroxy-4-nitroaniline) via fluorescence in CH_2Cl_2/DMSO (v:v = 199:1) at ambient temperature.

The free compound **2** (5×10^{-6} M) displayed an emission at 390 nm (λ_{ex} = 318 nm; the emission and excitation slits were all 15 nm), as shown in Figure 1. After adding 10 equiv of *o*-nitrophenol, *p*-nitrophenol, nitrobenzene, *m*-dinitrobenzene, *m*-nitroaniline, *p*-nitroaniline, *p*-nitrotoluene, 2,4-dinitrotoluene, and 2-hydroxy-4-nitroaniline to the solutions of **2**, no

https://doi.org/10.1021/acsomega.2c07587
ACS Omega 2023, 8, 6869−6874

Scheme 2. Interactions of *p*-DNB with 2

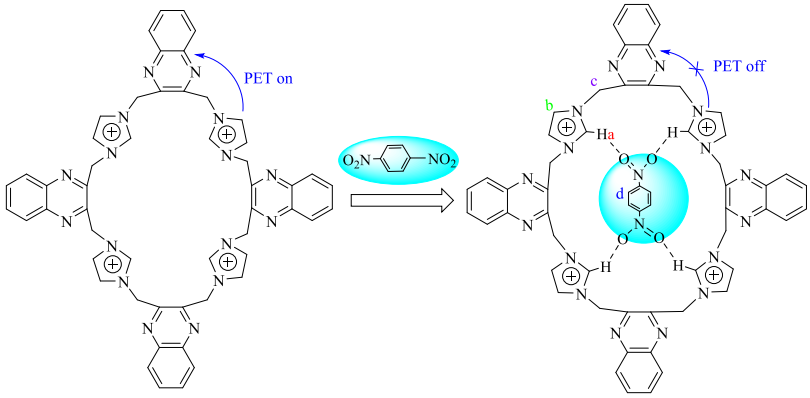

remarkable alteration of fluorescence was found. When an equal number of *p*-dinitrobenzene (*p*-DNB) was added, the fluorescence intensity of **2** significantly enhanced at 390 nm. This indicated that **2** was of a high selectivity to *p*-DNB, and it can be used as a chemosensor to distinguish *p*-DNB from other nitro compounds. Additionally, the UV spectra of compound **2** in the presence and absence of *p*-DNB were also measured (Figure S1). The absorption of **2** at 300−350 nm obviously increased after adding *p*-DNB to the solution of **2**, and this result further indicated that **2** has good selectivity for *p*-DNB.

As shown in Figure 2, the fluorescence intensities of **2** at 390 nm enhanced gradually with the increasing $C_{p\text{-DNB}}$ in the fluorescence titration experiments. While the ratio of $C_{p\text{-DNB}}/C_2$ changed from 0 to 12 ($C_{p\text{-DNB}}$ and C_2 were the concentrations of *p*-DNB and **2**, respectively), the fluorescence intensity enhanced little by little, as shown in the inset of Figure 2. When this ratio was more than 12, the tendency of enhancement of fluorescence intensity became slow until unchanged. The enhancing behavior of *p*-DNB on the fluorescence of **2** followed the Stern−Volmer equation (eq 1)

$$F_0/F = 1 + K_{SV}C_{p-DNB} \quad (1)$$

where F and F_0 are the fluorescence intensities of **2** in the presence and absence of *p*-DNB, respectively. K_{SV} is the association constant. K_{SV} for **2**·*p*-DNB is gotten as 2.9×10^4 M^{-1} ($R = 0.992$) by calculation, and the linear range is 0−6.0×10^{-6} M, as shown in Figure S2. The detection limit of **2** to *p*-DNB is gotten as 1.3×10^{-7} mol/L through calculation (Figure S3), and this value is in the medium position while comparing with the values in the literatures (from 6.1×10^{-5} to 1.5×10^{-8} mol/L).[23−25]

In Job's plot (Figure 3), χ is the molar fraction of **2** under a fixed overall concentration (5.0×10^{-6} M), and ΔI is the discrepancy of luminescence intensity with and without *p*-DNB. When χ is 0.5, $\chi\Delta I$ reaches its maximum value. This displays that the stoichiometric ratio between *p*-DNB and **2** is 1:1.

To further understand the selective capability of **2** to *p*-DNB, competitive experiments were performed. First, 10 equiv of different nitro compounds (*p*-nitrophenol, *o*-nitrophenol, nitrobenzene, *m*-dinitrobenzene, *m*-nitroaniline, *p*-nitroaniline, *p*-nitrotoluene, 2,4-dinitrotoluene, and 2-hydroxy-4-nitroaniline) was mixed with **2** (5×10^{-6} mol/L). Then, 10 equiv of *p*-DNB was added. No remarkable disturbance was observed (Figure S4). The results showed that **2** can discriminate *p*-DNB from other nitro compounds.

3.3. Interactions of *p*-DNB with 2. Through analyzing the structure of **2**, it was found that the H atom is the most possible bonding site for *p*-DNB. To gain detailed information about the bonding pattern of **2** and *p*-DNB, we conducted ^{1}H NMR titration tests in DMSO-d_6 (Figure 4). Upon the addition of 1.0 equiv of *p*-DNB (Figure 4v), the proton signals of *H*a and *H*d shifted downfield by 0.04 and 0.02 ppm, the signals of *H*b and *H*c moved upfield by about 0.02 ppm, while the other proton signals hardly changed. These alterations showed that *p*-DNB was held by the H atoms through C−H···O H bonds (Scheme 2). Besides, the signals of *H*a−*H*d had no obvious shifts upon adding more *p*-DNB (Figure 4vi), and this indicated that *p*-DNB and **2** had a 1:1 complexation.

In the mass spectrum of **2**·*p*-DNB (Figure S5), m/z (265.1683) of $[(\mathbf{2} + p\text{-DNB} - 4PF_6^-)/4]^+$ was found (the theoretical value is 265.2801), and this provided another evidence for the formation of a 1:1 complexation between **2** and *p*-DNB. This result was in line with the findings in Job's plot experiment. In the infrared spectra (Figure S6), the ν(C−N) absorption bands moved from 1165 cm^{-1} in free *p*-DNB to 1156 cm^{-1} in **2**·*p*-DNB, the ν(N═O) absorption bands moved from 1342 cm^{-1} in free *p*-DNB to 1328 cm^{-1} in **2**·*p*-DNB, and the ν(C−H) absorption bands moved from 3120 and 838 cm^{-1} in free *p*-DNB to 3113 and 826 cm^{-1} in **2**·*p*-DNB.

Through the comprehensive consideration of the structure of **2**, ^{1}H NMR titration, MS, and IR analyses, the bonding force of **2** and *p*-DNB is observed to have originated mostly from C−H···O H bonds. Each imidazolium in **2** is an electron-donating part as it includes an electron-rich π_5[7] bond, and the nitro group in *p*-DNB is an electron-withdrawing group. When *p*-DNB was held by **2**, the photoinduced *electron transfer* (PET) process from imidazolium to quinoxaline was turned off because of the effect of the nitro group.[26] As a consequence, the fluorescence intensity of **2** increased significantly. Additionally, we tried to cultivate a single crystal of **2**·*p*-DNB but did not succeed.

4. CONCLUSIONS

In sum, one macrocyclic tetra-imidazolium salt **2** based on quinoxaline was prepared and characterized, in which one 26-membered macrocycle was constructed by four imidazolium, four quinoxaline, and eight methylene groups. Macrocycle **2** has a special selectivity to the detection of *p*-DNB, and the large K_{SV} value (2.9×10^4 M^{-1}) showed that there was a strong acting force between the host and guest. The low detection limit (1.3×10^{-7} mol/L) showed that there was high sensitivity in the detection of the host to guest. Hence, **2**

https://doi.org/10.1021/acsomega.2c07587
ACS Omega 2023, 8, 6869−6874

can effectively distinguish *p*-DNB from other nitro compounds via the fluorescence method.

Recently, our research group reported another macrocyclic tetra-imidazolium salt based on fluorene and its recognition performance for *p*-nitroaniline.[22] Through comparison, the similarity of these two macrocycles in the literature and in this paper is that they all contain four imidazolium groups. However, these two macrocycles have some differences, for example: (i) their sizes are different (30-membered in the literature and 28-membered in this paper); (ii) their degree of distortion is different, and the distortion degree of the macrocycle in the literature is larger due to the presence of two flexible propylene groups; (iii) the hydrogen atoms on the benzene ring of the macrocycle in the literature participated in binding to the guest but not in this paper. As a result, these two macrocycles recognized different guests (*p*-nitroaniline in the literature and *p*-dinitrobenzene in this paper). Further investigations about the preparation and detection of new imidazolium salts are in progress.

■ ASSOCIATED CONTENT

Supporting Information

The Supporting Information is available free of charge at https://pubs.acs.org/doi/10.1021/acsomega.2c07587.

Figures for **2**, *p*-DNB, and **2**•*p*-DNB and NMR spectra for all intermediates and compound **2** (PDF)

■ AUTHOR INFORMATION

Corresponding Author

Qing-Xiang Liu − *Tianjin Key Laboratory of Structure and Performance for Functional Molecules, College of Chemistry, Tianjin Normal University, Tianjin 300387, P. R. China;* orcid.org/0000-0001-7824-3318; Email: tjnulqx@163.com

Authors

Zhi-Xiang Zhao − *Tianjin Key Laboratory of Structure and Performance for Functional Molecules, College of Chemistry, Tianjin Normal University, Tianjin 300387, P. R. China*

Yuan-Yuan Wu − *Tianjin Key Laboratory of Structure and Performance for Functional Molecules, College of Chemistry, Tianjin Normal University, Tianjin 300387, P. R. China*

Dong-Xue Zhao − *Tianjin Key Laboratory of Structure and Performance for Functional Molecules, College of Chemistry, Tianjin Normal University, Tianjin 300387, P. R. China*

Complete contact information is available at: https://pubs.acs.org/10.1021/acsomega.2c07587

Notes

The authors declare no competing financial interest.

■ ACKNOWLEDGMENTS

The financial support for this work was from the National Natural Science Foundation of China (No. 21572159) and Tianjin Natural Science Foundation (No. 18JCZDJC99600).

■ REFERENCES

(1) Liu, Q. X.; Sun, X. F.; Zhao, D. X.; Zhao, Z. X.; Liu, R.; Lv, S. Z. Selective recognition of m-dinitrobenzene based on NHC silver(I) macrometallocycle. *Sens. Actuators B: Chem.* **2017**, *249*, 203−209.

(2) Chakraborty, G.; Mandal, S. K. Design and development of fluorescent sensors with mixed aromatic bicyclic fused rings and pyridyl groups: solid mediated selective detection of 2,4,6-trinitrophenol in water. *ACS Omega* **2018**, *3*, 3248−3256.

(3) Xie, S.; Li, F.; Liu, F.; Xu, Q.; Zhang, X. Tough lanthanide luminescent hydrogel for nitroaromatics detection. *J. Rare Earths* **2022**, DOI: 10.1016/j.jre.2022.10.001.

(4) Lemaire, A.; Hapiot, P.; Geneste, F. Ti-catalyst biomimetic sensor for the detection of nitroaromatic pollutants. *Anal. Chem.* **2019**, *91*, 2797−2804.

(5) Cao, X. L.; Luo, L.; Zhang, F.; Miao, F. J.; Tian, D. M.; Li, H. B. Synthesis of a deep cavity calix[4] arene by four fold Sonogashira cross-coupling reaction and selective fluorescent recognition toward p-nitrophenol. *Tetrahedron Lett.* **2014**, *55*, 2029−2032.

(6) Xiao, Y.; Wang, Y.; You, Z. X.; Guan, Q. L.; Xing, Y. H.; Bai, F. Y.; Sun, L. X. Self-assembled Cd-MOF material supported by a triazine skeleton: stimuli response to traces of nitroaromatics and amines. *Cryst. Growth Des.* **2022**, *22*, 6967−6976.

(7) Li, J.; Liang, Y.; Wu, S.; Zhang, Y.; Zhu, M.; Gao, E. A novel Zn metal organic framework for the detection of *o*-nitrophenol, *m*-nitrophenol, *p*-nitrophenol. *Inorg. Chem. Commun.* **2022**, *143*, No. 109724.

(8) Li, H. S.; Wang, L. Y.; Wang, Y.; Bai, F. Y.; Xing, Y. H.; Shi, Z. Construction of uranyl MOF based on flexible triazine multi-carboxylate ligand and fluorescence response to nitro compounds. *Inorg. Chim. Acta* **2022**, *542*, No. 121116.

(9) Fernandes, P. F.; Bhasin, H.; Kashyap, P.; Mishra, D. R. CTV based sensor for the rapid detection of nitro toluene with computational studies and molecular modelling. *J. Fluoresc.* **2022**, *32*, 1279−1288.

(10) You, Z. X.; Zeng, G.; Bai, F. Y.; Xing, Y. H. Self-recovering ultraviolet-sensitive photochromic naphthalenediimide-based coordination networks: rapid fluorescence recognition of *p*-substituted nitrobenzenes. *J. Mater. Chem. C* **2021**, *9*, 14921−14937.

(11) Mu, R. P.; Shi, H. L.; Yuan, Y.; Karnjanapiboonwong, A.; Burken, J. G.; Ma, Y. F. Fast separation and quantification method for nitroguanidine and 2,4-dinitroanisole by ultrafast liquid chromatography-tandem mass spectrometry. *Anal. Chem.* **2012**, *84*, 3427−3432.

(12) Berg, M.; Bolotin, J.; Hofstetter, T. B. Compound-specific nitrogen and carbon isotope analysis of nitroaromatic compounds in aqueous samples using solid-phase microextraction coupled to GC/IRMS. *Anal. Chem.* **2007**, *79*, 2386−2393.

(13) Salinas, Y.; Martinez-Manez, R.; Marcos, M. D.; Sancenon, F.; Costero, A. M.; Parra, M.; Gil, S. Optical chemosensors and reagents to detect explosives. *Chem. Soc. Rev.* **2012**, *41*, 1261−1296.

(14) Sun, L. B.; Xing, H. Z.; Xu, J.; Liang, Z. Q.; Yu, J. H.; Xu, R. R. A novel (3,3,6)-connected luminescent metal-organic framework for sensing of nitroaromatic explosives. *Dalton Trans.* **2013**, *42*, 5508−5513.

(15) Nagarkar, S. S.; Joarder, B.; Chaudhari, A. K.; Mukherjee, S.; Ghosh, S. K. Highly selectively detection of nitro explosives by a luminescent metal-organic framework. *Angew. Chem., Int. Ed.* **2013**, *52*, 2881−2885.

(16) Kim, T. K.; Lee, J. H.; Moon, D.; Moon, H. R. Luminescent Li-based metal-organic framework tailored for the selective detection of explosive nitroaromatic compounds: direct observation of interaction sites. *Inorg. Chem.* **2013**, *52*, 589−595.

(17) Zhang, X.; Liu, L.; Wang, R.; Zhang, W.; Liu, Z.; Na, L.; Hua, R. PEI-capped $KMgF_3$:Eu^{2+} nanoparticles for fluorescence detection of nitroaromatics in municipal waste water. *Colloid. Surf. B* **2021**, *197*, No. 111379.

(18) Wang, Q.; Liu, D. J.; Cui, L. L.; Hu, X. L.; Wang, X. L.; Su, Z. M. A 3D pillared-layer metal-organic framework with fluorescence property for detection of nitroaromatic explosives. *New J. Chem.* **2019**, *43*, 963−969.

(19) Jia, Y. Y.; Li, T. J.; Yu, C. X.; Jiang, B.; Yao, C. S. A facile one-pot synthesis of 2,3-diarylated benzo[*b*] furans *via* relay NHC and palladium catalysis. *Org. Biomol. Chem.* **2016**, *14*, 1982−1987.

(20) Que, Y. L.; Lu, Y. N.; Wang, W. J.; Wang, Y. H.; Wang, H. T.; Yu, C. X.; Li, T. J.; Wang, X. S.; Shen, S. D.; Yao, C. S. *Chem. − Asian J.* **2016**, *11*, 678−681.

(21) Pape, T.; Hahn, F. E. Synthesis of polynuclear Ag(I) and Au(I) complexes from macrocyclic tetraimidazolium salts. *Dalton Trans.* **2013**, *42*, 7330−7337.
(22) Bian, Q. Q.; Liu, Y. J.; Zhao, Z. X.; Wu, H.; Liu, Q. X. Macrocyclic tetra-imidazolium salt sensor for *p*-nitroaniline sensing. *Tetrahedron* **2022**, *128*, No. 133113.
(23) Shen, A. Q.; Yan, Z. W.; Jia, L. H.; Yang, R.; Wang, J. P.; Guo, X. F. Selective detection of m-dinitrobenzene by naphthalimide fluorescent fiber sensor. *Chin. J. Anal. Lab.* **2020**, *39*, 844−888.
(24) Qin, P.; Yang, H. H.; Zhao, X. X.; Qu, W. J.; Yao, H.; Wei, T. B.; Lin, Q.; Shi, B. B.; Zhang, Y. M. A supramolecular polymer network constructed by pillar[5] arene based host-guest interactions and its application in nitro explosive detection. *J. Inclusion Phenom. Macrocyclic Chem.* **2022**, *102*, 295−302.
(25) Qu, Y. H.; Liu, Y.; Zhou, T. S.; Shi, G. Y.; Jin, L. T. Electrochemical sensor prepared from molecularly imprinted polymer for recognition of 1,3-Dinitrobenzene (DNB). *Chin. J. Chem.* **2009**, *27*, 2043−2048.
(26) Escudero, D. Revising intramolecular photoinduced electron transfer (PET) from first-principles. *Acc. Chem. Res.* **2016**, *49*, 1816−1824.

https://doi.org/10.1021/acsomega.2c07587
ACS Omega 2023, 8, 6869−6874